Journal of Zhejiang University-SCIENCE A (Applied Physics & Engineering)
ISSN 1673-565X (Print); ISSN 1862-1775 (Online)
www.zju.edu.cn/jzus; www.springerlink.com
E-mail: jzus@zju.edu.cn

Analysis of streamwise conduction in forced convection of microchannels using fin approach

Suhandran MUNIANDY[1,2], Yew Mun HUNG[‡3]

([1]*Faculty of Engineering and Technology, Multimedia University, 75450 Melaka, Malaysia*)

([2]*Infineon Technologies Sdn Bhd, Batu Berendam, 75350 Melaka, Malaysia*)

([3]*School of Engineering, Monash University, 46150 Bandar Sunway, Malaysia*)

E-mail: hbksuhan@yahoo.com; hungyewmun@gmail.com

Received June 20, 2010; Revision accepted Oct. 22, 2010; Crosschecked Aug. 1, 2011

Abstract: The effects induced by streamwise conduction on the thermal characteristics of forced convection for single-phase liquid flow in rectangular microchannel heat sinks under imposed constant wall temperature have been studied. By employing the fin approach in the first law of analysis, models with and without streamwise conduction term in the energy equation were developed for hydrodynamically and thermally fully-developed flow under local thermal non-equilibrium for the solid and fluid phases. These two models were solved to obtain closed form analytical solutions for the fluid and solid temperature distributions and the analysis emphasized details of the variations induced by the streamwise conduction on the fluid temperature distributions. The effects of the Peclet number, aspect ratio, and thermal conductivity ratio on the thermal characteristics of forced convection in microchannel heat sinks were analyzed and discussed. This study reveals the conditions under which the effect of streamwise conduction is significant and should not be neglected in the forced convective heat transfer analysis of microchannel heat sinks.

Key words: Streamwise conduction, Fin approach, Microchannel heat sink
doi:10.1631/jzus.A1000289 **Document code:** A **CLC number:** TK12

1 Introduction

Rapid development in the semiconductor technology has led to a tremendous increase in power density encountered in electronic devices and chips. In light of the effectiveness rendered in the enhancement of heat dissipation in electronics cooling, microchannel heat sinks have received much attention since they were first proposed by Tuckerman and Pease (1981). Hence, a large number of studies have been carried out to investigate the heat and fluid flow characteristics to primarily evaluate the thermal performance of microchannel heat sink. A number of reviews on the heat transfer and fluid flow characteristics of microchannels have been well-documented (Duncan and Peterson, 1994; Ho and Tai, 1998; Gad-el-Hak, 1999; Garimella and Sobhan, 2003; Hetsroni *et al*., 2005a; 2005b).

In the theoretical studies on microchannel heat sinks, the fin approach is one of the analytical approaches adopted due to its effectiveness and relative simplicity in the analysis of the transport phenomena, based on the assumption of 1D heat conduction along the fin or the channel plate height. This method further simplifies the heat transfer analysis by considering a constant heat transfer coefficient and a uniform fluid temperature in the transverse direction of the flow. Knight *et al*. (1991) analyzed the heat transfer in microchannel heat sinks through a model based on the fin approach, and by employing empirical correlation in the analysis, and it was found that the microchannel heat sink thermal resistance can be reduced by 35% compared to that obtained by Tuckerman and Pease (1981). Zhao and Lu (2002) compared the analytical solutions obtained from both

‡ Corresponding author

the fin approach and the porous medium model and claimed that the fin approach overestimates the heat transfer due to the assumption of uniform transverse fluid temperature. While the porous medium model is deemed to be more accurate in the analysis of the thermal performance of microchannel heat sink, it is incapable of capturing the effect of streamwise conduction when analytical solutions are desired, such as Kim and Kim (1999), Zhao and Lu (2002), Kim and Kim (2006) and Chen (2007). Most existing analytical studies on microchannel heat sink neglected the effect of streamwise conduction despite that this effect is justified to significantly affect the heat transport rate in proximity to the entrance region of the fluid flow for conventional size channels (Nguyen, 1992; Lahjomri and Oubarra, 1999; Weigand and Lauffer, 2004). Due to the fact that the characteristic time of convection and conduction are comparable for flows with small Peclet number, the streamwise conduction becomes indispensable. Michelsen and Villadsen (1974) investigated this problem and recommended the Nusselt number correlations for low values of the Peclet number, in which case the effect of the streamwise conduction is significant. As the internal flows in micro-scale devices are typically characterized by finite Peclet numbers, the incorporation of the effect of streamwise conduction is a necessity in the thermal analysis of microchannel heat sinks. However, these analyses, which normally involve Graetz-type problems with the inclusion of streamwise conduction, are inherently complicated as a result of the presence of the non-self-adjoint eigenvalue problem and the according non-orthogonal eigenfunctions (Deen, 1998). To characterize the streamwise conduction effect in microchannels, Hetsroni *et al*. (2005b) adopted an analytical model by averaging the fluid temperature over the microchannel cross-section and using a 1D energy equation for the flow of incompressible fluid with constant physical properties. They pointed out that the presence of streamwise conduction induces an increasing difference between the wall-fluid temperature and a decreasing value of the Nusselt number within the entrance section. With the inclusion of the streamwise conduction term in the energy equation, Zhao and Lu (2002) conducted numerical analyses by using a finite difference scheme on the porous medium model for microchannel heat sinks to confirm the accuracy of the analytical solutions by neglecting the streamwise conduction. Husain and Kim (2008) performed numerical optimizations of microchannel heat sinks with the help of surrogate analysis and an evolutionary algorithm. The streamwise conduction was included in their model of which the governing equations were solved using the commercial code ANSYS CFX 11.0. Several studies, which include the streamwise conduction effect, have been carried out on gaseous flow in microchannels. By considering axial conduction, rarefaction and viscous dissipation effects, Jeong and Jeong (2006) employed an eigenfunction expansion to solve the energy equation for hydrodynamically-developed and thermally-developing flow with isothermal and isoflux boundary conditions. Cetin *et al*. (2008) numerically solved a similar problem with the isothermal boundary condition using a finite difference method. Under hydrodynamically and thermally fully-developed conditions and with the presence of streamwise conduction, Hadjiconstantinou and Simek (2002) employed the slip-flow theory and direct simulation Monte Carlo to evaluate the Nusselt number for different ranges of the Knudsen number.

The present study focuses on the effects induced by the streamwise conduction on the thermal performance of microchannel heat sinks. An analytical model is proposed based on the fin approach for a rectangular microchannel heat sink with a single-phase incompressible fluid under hydrodynamically and thermally fully-developed flow conditions subjected to a constant wall temperature boundary condition. By comparing the models with and without the incorporation of streamwise conduction, and under local thermal non-equilibrium for the solid and fluid phases, the analysis emphasizes details of the variations incurred by the streamwise conduction on the fluid temperature distribution. The effects of the pertinent physical parameters, such as the Peclet number, thermal conductivity ratio, and aspect ratio of the microchannel heat sink, are investigated and discussed.

2 Mathematical formulation

In a microchannel heat sink, heat is removed primarily by conduction through the solid and dissipated by convection due to the flow of the fluid. The

microchannel heat sink (Fig. 1) consists of channels with height H, width a, length L, and the thickness of the channel plate is t. The unit cell of the heat sink under investigation is bound by the dotted lines. The bottom surface of the microchannel heat sink (y=0) is kept at constant temperature (T_w) and the top surface (y=H) is insulated. The temperatures of the fluid and the solid plate are assumed to have been properly integrated over the width of the channel and the thickness of the plate, respectively, to yield 2D averaged fluid temperature $T_f(x,y)$ and solid plate temperature $T_s(x,y)$. The adopted fin approach is based on 1D heat conduction along the height of the solid plate and the fin equation for the solid plate (Incropera *et al.*, 2007) is given by

$$\frac{\mathrm{d}^2T_s}{\mathrm{d}y^2}-\frac{2h}{k_s t}\left[T_s-T_f(x)\right]=0, \tag{1}$$

where k_s is the thermal conductivity of the solid plate, and h denotes the interfacial heat transfer coefficient.

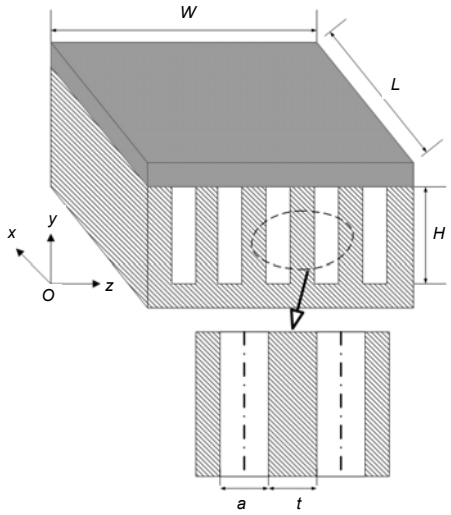

Fig. 1 Schematic diagram of the microchannel heat sink with geometry definition

In the present model, the fluid temperature is further averaged over the height of the channel to yield the bulk mean temperature $T_f(x)$ over the rectangular cross-section. For hydrodynamically and thermally fully-developed laminar channel flow, this coefficient is related to the Nusselt number correlation proposed by Kim and Kim (1999) through the formula:

$$Nu_D=\frac{hD_h}{k_f}=2.253+8.164\left(\frac{\alpha}{\alpha+1}\right)^{3/2}, \tag{2}$$

where D_h=2aH/(a+H) is the hydraulic diameter of the rectangular channel, k_f is the thermal conductivity of fluid, and α=H/a is the channel aspect ratio. The appropriate thermal boundary conditions are expressed as

$$T_s(x,0)=T_w,\quad \left.\frac{\partial T_s}{\partial y}\right|_{y=H}=0. \tag{3}$$

The application of these boundary conditions on Eq. (1) yields the solid plate temperature distribution:

$$\begin{aligned}&T_s(x,y)\\&=T_f(x)+\frac{\cosh\left[\sqrt{2Bi}(H-y)/t\right]}{\cosh(\sqrt{2Bi}H/t)}\left[T_w-T_f(x)\right],\end{aligned} \tag{4}$$

where Bi is the Biot number, which can be related to the Nusselt number as

$$Bi=\frac{ht}{k_s}=\frac{\kappa Nu_D(1+\alpha)}{2\alpha\varepsilon^2/(1-\varepsilon)^2}, \tag{5}$$

where κ is the effective thermal conductivity ratio and ε is the porosity which defines the working fluid volume fraction of the microchannel heat sink, which are, respectively, given by

$$\kappa=\frac{\varepsilon k_f}{(1-\varepsilon)k_s}, \tag{6}$$

$$\varepsilon=\frac{a}{a+t}. \tag{7}$$

The heat transfer rate per unit length of the channel from the solid plate to the working fluid can be determined from Fourier's law of heat conduction:

$$\begin{aligned}\dot{q}(x)&=-k_s t\left.\frac{\mathrm{d}T_s}{\mathrm{d}y}\right|_{y=0}\\&=k_s\sqrt{2Bi}\tanh\left(\frac{\sqrt{2Bi}H}{t}\right)\left[T_w-T_f(x)\right].\end{aligned} \tag{8}$$

To derive the energy equation for the working fluid inside the microchannel heat sink, we apply the

conservation of energy to the infinitesimal control volume depicted in Fig. 2 and the ordinary differential equation obtained is expressed as

$$-k_f aH\frac{d^2T_f(x)}{dx^2}+\rho c_p u_m aH\frac{dT_f(x)}{dx}=\left[k_s\sqrt{2Bi}\tanh(\sqrt{2Bi}H/t)+ha\right]\left[T_w-T_f(x)\right], \tag{9}$$

where u_m is the mean velocity, ρ is the density, and c_p is the specific heat capacity.

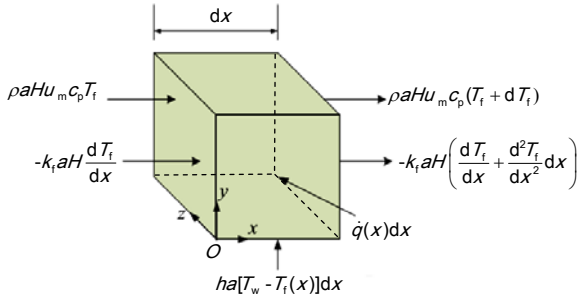

Fig. 2 Differential control volume for the derivation of energy equation in the liquid domain

In arriving at the above equation, the fluid flow is assumed to be unidirectional and hydrodynamically and thermally fully-developed with u_m. The thermophysical properties of the fluid, i.e., ρ, c_p, and k_f, are assumed to be independent of temperature. With the fluid temperature T_0 at the entrance and the assumption that the exit of the microchannel is connected to an adiabatic section, the corresponding thermal boundary conditions for the fluid are written as

$$T_f(0)=T_0,\quad \left.\frac{dT_f}{dx}\right|_{x=L}=0. \tag{10}$$

By introducing the following dimensionless variables:

$$X=\frac{x}{L},\quad \theta_f(X)=\frac{T_w-T_f(x)}{T_w-T_0}, \tag{11}$$

the governing equation of Eq. (9) and the thermal boundary conditions of Eq. (10) are nondimensionalized, respectively, as

$$C_1\frac{d^2\theta_f}{dX^2}-C_2\frac{d\theta_f}{dX}=C_3\theta_f, \tag{12}$$

$$\theta_f(0)=1,\quad \left.\frac{d\theta_f}{dX}\right|_{X=1}=0, \tag{13}$$

where the coefficients C_1, C_2 and C_3 are, respectively, given by

$$C_1=\frac{\gamma^2}{\alpha}, \tag{14}$$

$$C_2=Pe_D\gamma\left(\frac{\alpha+1}{2\alpha}\right), \tag{15}$$

$$C_3=\frac{\varepsilon\sqrt{2Bi}}{\kappa(1-\varepsilon)}\tanh\left(\frac{\varepsilon\alpha\sqrt{2Bi}}{1-\varepsilon}\right)+\frac{(\alpha+1)Nu_D}{2\alpha}, \tag{16}$$

where γ is the channel aspect ratio of the microchannel and $\gamma=H/L$, and the Peclet number is

$$Pe_D=\frac{\rho c_p u_m D_h}{k_f}. \tag{17}$$

Solving Eq. (12) together with the boundary conditions of Eq. (13) yields the closed form analytical solution for the dimensionless fluid temperature profile as

$$\begin{aligned}\theta_f(X)=2C_1\{&(\omega+\lambda)\exp[\omega+\lambda+(\omega-\lambda)X]\\&-(\omega-\lambda)\exp[\omega-\lambda+(\omega+\lambda)X]\}/\\&\{2C_1\lambda[\exp(\omega+\lambda)+\exp(\omega-\lambda)]\\&+C_2[\exp(\omega+\lambda)-\exp(\omega-\lambda)]\},\end{aligned} \tag{18}$$

where

$$\omega=\frac{C_2}{2C_1}, \tag{19}$$

$$\lambda=\frac{\sqrt{C_2^2+4C_1C_3}}{2C_1}. \tag{20}$$

For the case when streamwise conduction term is neglected in the energy equation, the dimensionless average fluid temperature profile is given by

$$\theta_f^*(X)=\exp\left\{-\frac{Nu_D}{\gamma Pe_D}\times\left[1+\left(\frac{1-\varepsilon}{\varepsilon}\right)\sqrt{\frac{2}{Bi}}\tanh\left(\sqrt{2Bi}\frac{\varepsilon\alpha}{1-\varepsilon}\right)\right]X\right\}. \tag{21}$$

Hereafter, for the purpose of comparison of results, the model with the streamwise conduction term incorporated into the energy equation is denoted as Model 1; and that without the streamwise conduction term as Model 2 (with a superscript *).

3 Results and discussion

The major difference between the macro-scale and micro-scale liquid flows arises from the significance of the effects of streamwise conduction and viscous dissipation in the latter. Hetsroni *et al.* (2005b) discussed the effect of viscous dissipation which may lead to drastic change of flow and temperature fields in microchannels under certain conditions, particularly for fluids with low specific-heats and high viscosities (Koo and Kleinstreuer, 2004). Significant viscous dissipation effects have been observed for a large Brinkman number, which is defined as the ratio of the heat generation due to viscous forces to the heat transferred from the wall to the fluid (Hung, 2009). The large Brinkman number is characterized by fluids with low thermal conductivities and high viscosities and for flows in a long channel with a small hydraulic diameter. Employing water as working fluid in microchannels, Tso and Mahulikar (1998; 1999; 2000) revealed that the experimental data in laminar flow regime correlate well with the Brinkman number. However, they discovered that small values of the Brinkman number do not considerably affect the Nusselt number when the Reynolds number and the Prandtl number do not change significantly. Typically, the viscous dissipation has a pronounced impact on the convective heat transfer characteristics when the Reynolds number and the Prandtl number are high (Koo and Kleinstreuer, 2004). Under such circumstance, the Peclet number is also high as the Peclet number is the product of the Reynolds number and the Prandtl number. On the other hand, as justified by previous studies such as Michelsen and Villadsen (1974), Nguen (1992) and Weigand and Lauffer (2004), the streamwise conduction effect is only significant at low Peclet number, in which case the Reynolds number and the Prandtl number are consequently low. Inasmuch as the present study is devoted to the streamwise effect on convective heat transfer in microchannels at low Peclet number, the effect of viscous dissipation can be reasonably neglected.

In Eqs. (14)–(21), the dimensionless fluid temperature is dependent on the pertinent physical parameters such as the Peclet number Pe_D, thermal conductivity ratio κ, and aspect ratio of the microchannel heat sink, α, hence the analysis of the temperature distributions is based on the variations of such parameters. Fig. 3 illustrates the effect of Pe_D variation on the dimensionless fluid temperature distribution for fixed values of aspect ratios (α=1 and γ=0.1), thermal conductivity ratio (κ=0.004) and porosity (ε=0.5). To characterize the total amount of heat transported by the fluid, it is instructive to consider Eq. (12), the differential equation governing the dimensionless fluid temperature distribution. Integrating Eq. (12) over the entire length of the microchannel and using the boundary conditions in Eq. (13) gives

$$-C_1 \left.\frac{\mathrm{d}\theta_\mathrm{f}}{\mathrm{d}X}\right|_{X=0} + C_2\left[1-\theta_\mathrm{f}(1)\right] = C_3\int_0^1 \theta_\mathrm{f}\,\mathrm{d}X. \qquad (22)$$

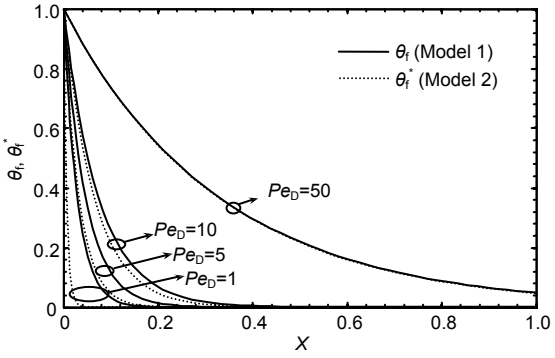

Fig. 3 Comparison of dimensionless fluid temperature distributions between Model 1 and Model 2 along the axial direction of the channel at different Pe_D with α=1, γ=0.1, κ=0.004 and ε=0.5

The first term on the left-hand side of Eq. (22) concerns the dimensionless form of the heat transport due to axial conduction, while the second term is referred to as the dimensionless form of convective heat transfer. The integral on the right-hand side of Eq. (22) is proportional to the total heat transfer from the solid plate and the base wall, which is absorbed by the fluid and transported through axial conduction and convection. Therefore, the area under the curve of the dimensionless fluid temperature distribution serves as a representation of the total amount of heat absorption of the fluid throughout the channel length.

To characterize the role of streamwise conduction, attention is focused on the comparison between

the models with and without considering streamwise conduction by analyzing the deviations induced in the fluid temperature distributions. Fig. 3 shows the dimensionless fluid temperature distributions for both models at different Pe_D. From Model 1, with streamwise conduction, one can perceive that the temperature gradient becomes steeper as Pe_D reduces, implying that the fluid temperature $T_f(x)$ rises more rapidly along the channel as Pe_D decreases. The dimensionless fluid temperature distribution reaches zero at about X=0.2 when Pe_D=1, showing that the fluid flows isothermally at $T_f(x)=T_w$ without absorbing heat for the remaining of the channel as T_w is the maximum temperature that the fluid can reach. For larger Pe_D=50, the dimensionless fluid temperature distribution remains above zero throughout the entire channel length, and hence the fluid absorbs heat for the entire channel length. Therefore, it shows that reduction in the Peclet number shortens the distance in which the heat transfer to the fluid takes place. By comparing the two models with and without streamwise conduction, it is observed that the discrepancy is larger for small Pe_D and decreases with increasing Pe_D. The dimensionless fluid temperature distribution obtained from Model 1 deviates noticeably from that obtained from Model 2 at Pe_D=1, indicating that the existence of heat transfer due to streamwise conduction leads to an increasing difference between wall-fluid temperature within the entrance section. However, for larger Peclet number Pe_D=50, the dimensionless temperature distributions from Model 1 are shown to match well with those from Model 2. Thus, for hydrodynamically and thermally fully-developed flow, it implies that the fluid axial conduction induces pronounced effect only when Pe_D is sufficiently small, and the streamwise conduction can be neglected in the analysis of heat transfer for large Pe_D. The fluid reaches thermal equilibrium with the base wall at the axial location which is denoted as the equilibrium point where the dimensionless fluid temperature is zero. For Pe_D=1, the distance from the entrance of the channel to the equilibrium point of Model 1 appears to be longer than that of Model 2. Therefore, the streamwise conduction causes the fluid to reach thermal equilibrium with the base wall at the axial location farther from the channel inlet, and the presence of the streamwise conduction increases the distance in which the heat transfer to the fluid takes place. In other words, fluid absorbs heat for a longer distance along the channel due to the presence of the streamwise conduction.

To investigate the effect of aspect ratio α, Fig. 4 depicts the comparison of the dimensionless fluid temperature distributions between Model 1 and Model 2 at different α with γ=0.1, ε=0.5, κ=0.004 for Pe_D=1 and Pe_D=10. When Pe_D=1, the fluid temperatures distributions of both models deviate noticeably from each other for different α. Additionally, the discrepancy of the dimensionless fluid temperatures between both models reduces as α increases. When Pe_D=1, it is observed that the dimensionless fluid temperature distributions of Model 1 are in good agreement with those of Model 2 for different α, showing that Model 2 in the energy equation predicts the fluid temperature very close to that of Model 1. On the other hand, when α is increased, the equilibrium points for both models shift toward the entrance of the microchannel and the total heat transported by the fluid decreases, as the area under the curve of the dimensionless fluid temperature distribution is susceptible to shrinkage. Thus, an increase in α shortens the distance in which the heat transfer to the fluid takes place for both models. This is attributable to the fact that the interfacial heat transfer coefficient between solid and fluid is related to the Nusselt number correlation, which is given in Eq. (2), is a function of α. Since the Nusselt number increases with α, it can be deduced that as α increases, the convective heat transfer rate increases, and hence the effect of streamwise conduction becomes less significant.

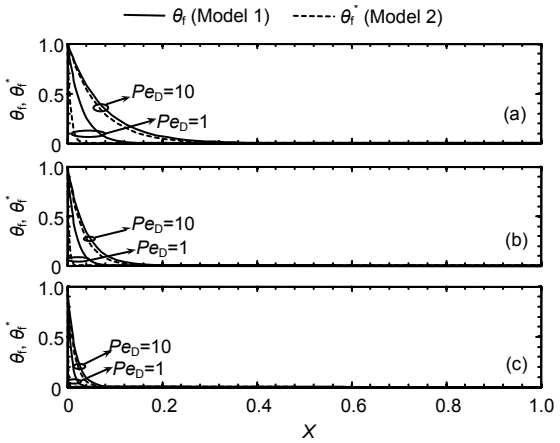

Fig. 4 Comparison of dimensionless fluid temperature distributions between Model 1 and Model 2 along the axial direction of the channel with Pe_D=1 and Pe_D=10 with γ=0.1, κ=0.004 and ε=0.5

(a) α=1; (b) α=2; (c) α=3

Fig. 5 shows the dimensionless fluid temperature distributions of Model 1 and Model 2, with κ being the parameter, for Pe_D=1 and Pe_D=10. It is observed that the dimensionless fluid temperature distributions from both models exhibit significant discrepancy for different κ when the Peclet number is sufficiently small (Pe_D=1). However, the dimensionless fluid temperature distributions as well as the amount of heat transfer by the fluid of both models are insensitive to the variation of κ. When the Peclet number increases to Pe_D=10, the dimensionless fluid temperature distributions profiles of Model 1 for different κ are shown to be close to those of Model 2. This can be explained by the fact that when κ is varied by fixing other parameters including the Peclet number and porosity ε, in which case the thermal conductivity of solid, k_s, is the only parameter changed, as seen from the definition of κ in Eq. (6). As the heat transfer characteristics of the working fluid are not affected by the thermal conductivity of the solid under the imposition of constant wall temperature, variation of κ renders no effect on the fluid temperature distribution. Therefore, the streamwise conduction incurs significant effect at any κ when only the Peclet number is sufficiently small. Similarly, for a given κ, the streamwise conduction shifts the equilibrium point towards the downstream region of the flow, showing that the distance from the entrance of the microchannel to the equilibrium point appears to be longer for Model 1 compared to that for Model 2, and subsequently the amount of heat transfer by the fluid increases with the incorporation of the streamwise conduction.

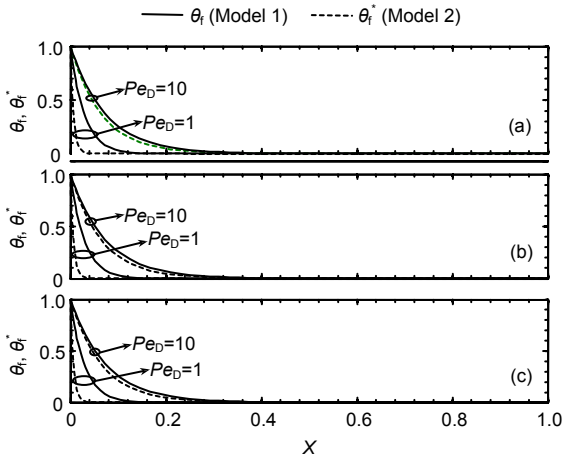

Fig. 5 Comparison of dimensionless fluid temperature distributions between Model 1 and Model 2 along the axial direction of the channel with Pe_D=1 and Pe_D=10, γ=0.1, ε=0.5 and α=1

(a) κ=0.0005; (b) κ=0.001; (c) κ=0.004

Based on the discussion in the preceding paragraphs, it is known that the Peclet number Pe_D is the definitive parameter that characterizes the significance of the streamwise conduction. To quantify the significance of the streamwise conduction, a parameter:

$$M=\frac{|F_{\text{cond}}|}{|F_{\text{conv}}|}, \tag{23}$$

which is the ratio of axial heat conduction $F_{\text{cond}}=-k_f\dfrac{\mathrm{d}T_f}{\mathrm{d}x}$, to heat convection $F_{\text{conv}}=\rho u_m c_p(T_f-T_0)$, of the fluid is defined, analogous to that introduced by Maranzana *et al.* (2004) for analyzing axial conduction in solid wall. In dimensionless form, the parameter can be expressed as

$$M=\left|\frac{2\gamma}{(\alpha+1)Pe_D(\theta_f-1)}\frac{\mathrm{d}\theta_f}{\mathrm{d}X}\right|. \tag{24}$$

Fig. 6 illustrates the variation of M along the axial direction of the microchannel γ=0.1, α=1, ε=0.5 and κ=0.004, with Pe_D being a parameter. For Pe_D=1, M is significantly large in the vicinity of the channel entrance. The order of magnitude of M is 10^2 in the vicinity of the channel entrance, indicating that the streamwise conduction dominates over the heat transport due to convection in the axial direction. When X increases, M decreases drastically, showing

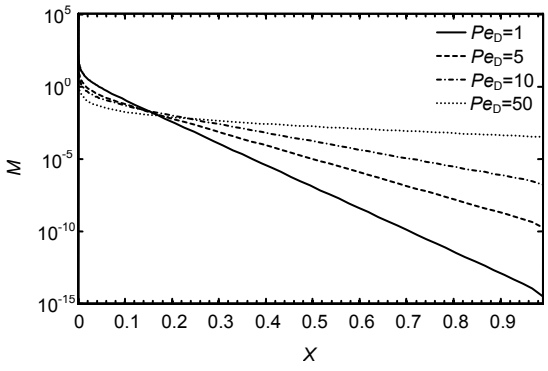

Fig. 6 Variation of M along the axial direction of the microchannel for γ=0.1, α=1, κ=0.004 and ε=0.5

that the convection heat transfer overcomes and dominates over the conduction heat transfer at a short distance from the entrance. Beyond the mid-section of the channel, M is substantially small and the heat transported by the fluid is mainly due to convection. For all values of Pe_D, the region where M is significantly large is confined to the channel entrance and shrinks as Pe_D increases. Therefore, the degree of significance of the effect of streamwise conduction decreases with increasing Pe_D.

3.1 Case study

To illustrate the effects of different combinations of solid wall and working fluid as well as different fluid velocity on the axial fluid temperature distribution, a case study based on known materials and dimensions of the microchannel heat sink is performed. The heat sink has dimensions of $a=t=H=100$ μm and the length $L=1$ mm. Two different types of working fluid: water and isobutene (R600a), and two different solid wall materials: copper ($k=401$ W/(m·K)) and chromium steel ($k=37.7$ W/(m·K)), constitute four different wall-fluid combinations. The bottom wall temperature remains at $T_w=60$ °C and the mean temperature at the inlet, T_0, is at 20 °C. All fluid properties are evaluated at the bulk mean fluid temperature $T_b=(T_0+T_1)/2$, where T_1 is the mean temperature at the exit. The thermophysical properties are obtained by Çengel (2006). With the incorporation of the effect of streamwise conduction, Fig. 7 depicts the fully-developed fluid temperature distribution for different wall-fluid combinations at two different values of fluid velocity. For the same working fluid, the variation of fluid temperature distribution is independent of the solid wall material under the imposition of constant wall temperature. This is consistent with the observation in Fig. 5 that fixing other parameters and varying κ does not render effect on the heat transfer characteristics of the working fluid. On the other hand, when different working fluids are employed, significant variations are induced on the temperature distribution. At a given velocity, it can be observed that water reaches thermal equilibrium with the base wall earlier than R600a, attributed to the fact that the Peclet number of the former is smaller than that of the latter. When the velocity is increased ten times, by fixing other parameters, the Peclet number is correspondingly increased to the same extent. In this case, the equilibrium point is shifted toward the downstream region of the flow and more heat energy can be absorbed by the working fluid when the fluid velocity is increased. Therefore, it can be concluded that the thermal performance of R600a is better than that of water and the amount of heat transport increases with circulation rate of the working fluid.

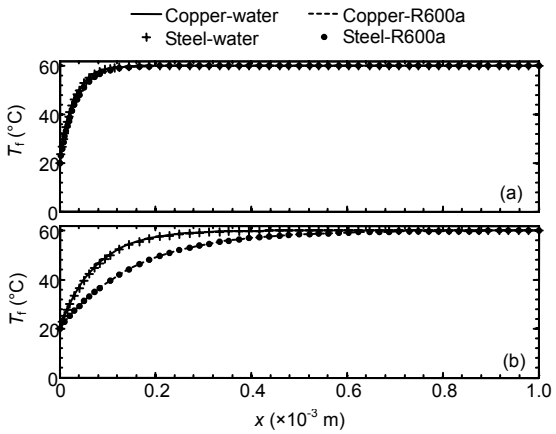

Fig. 7 Axial fluid temperature distributions of Model 1 for different solid-fluid combinations when T_w=60 °C and T_0=20 °C
(a) u_m=0.00152 m/s; (b) u_m=0.0152 m/s

For comparison between models with and without streamwise conduction, Fig. 8 plots the fluid temperature distributions for copper-water and copper-R600a microchannel heat sinks at $T_w=60$ °C and $T_0=20$ °C. At a given velocity, the effect of streamwise conduction is more pronounced in water than in R600a, due to the fact that the Peclet number of water is smaller than that of R600a. As expected, when the velocity is increased ten times (the Peclet number also increases to the same extent), the effect induced by the streamwise conduction diminishes and the heat transport in the working fluid is dominated by convective heat transfer.

4 Conclusions

When the streamwise conduction is taken into account, it is observed that the fluid temperature distribution is a strong function of the Peclet number. It is evident that the deviation of the fluid temperature distribution between the models with and without considering streamwise conduction effect increases as

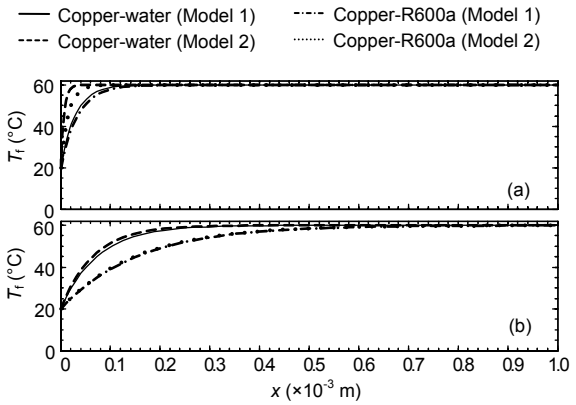

Fig. 8 Axial fluid temperature distributions of Model 1 and Model 2 for copper-water and copper-R600a combinations when T_w=60 °C and T_0=20 °C
(a) u_m=0.00152 m/s; (b) u_m=0.0152 m/s

the Peclet number decreases. Reduction in the Peclet number shortens the distance in which the heat transfer to the fluid takes place along the channel length. The fluid temperature distributions from both models exhibit significant discrepancy for different aspect ratio and thermal conductivity ratio when the Peclet number is sufficiently small. However, the fluid temperature distributions as well as the amount of heat transfer by the fluid of both models are insensitive to the variation of thermal conductivity ratio. It is shown that in the vicinity of the channel entrance, the streamwise conduction dominates over the heat transport due to convection in the axial direction but the reverse is true beyond a short distance from the entrance. Beyond the mid-section of the channel, the heat transported by the fluid is mainly due to convection and the degree of significance of the effect of streamwise conduction decreases with the increasing Peclet number. It can be concluded that the influence of streamwise conduction on the forced convective heat transfer in microchannel heat sink is significant albeit not dominant especially for a small Peclet number and in the vicinity of the entrance region.

References

Çengel, Y.A., 2006. Heat and Mass Transfer: A Practical Approach (3rd Ed.). McGraw-Hill, Singapore, p.854-858.

Cetin, B., Yazicioglu, A.G., Kakac, S., 2008. Fluid flow in microtubes with axial conduction including rarefaction and viscous dissipation. *International Communications in Heat and Mass Transfer*, **35**(5):535-544. [doi:10.1016/j.icheatmasstransfer.2008.01.003]

Chen, C.H., 2007. Forced convection heat transfer in microchannel heat sinks. *International Journal of Heat and Mass Transfer*, **50**(11-12):2182-2189. [doi:10.1016/j.ijheatmasstransfer.2006.11.001]

Deen, W.M., 1998. Analysis of Transport Phenomena. Oxford University Press, Oxford, p.392.

Duncan, A.B., Peterson, G.P., 1994. Review of microscale heat transfer. *Applied Mechanics Reviews*, **47**(9):397-428.

Gad-el-Hak, M., 1999. The fluid mechanics of microdevices —The freeman scholar lecture. *Journal of Fluid Engineering*, **121**(1):5-33. [doi:10.1115/1.2822013]

Garimella, S.V., Sobhan, C.B., 2003. Transport in microchannels—a critical review. *Annual Review of Heat Transfer*, **13**:1-50.

Hadjiconstantinou, N.G., Simek, O., 2002. Constant-wall-temperature Nusselt number in micro and nano-channels. *ASME Journal of Heat Transfer*, **124**(2):356-364. [doi:10.1115/1.1447931]

Hetsroni, G., Mosyak, A., Pogrebnyak, E., Yarin, L.P., 2005a. Fluid flow in micro-channels. *International Journal of Heat and Mass Transfer*, **48**(10):1982-1998. [doi:10.1016/j.ijheatmasstransfer.2004.12.019]

Hetsroni, G., Mosyak, A., Pogrebnyak, E., Yarin, L.P., 2005b. Heat transfer in micro-channels: Comparison of experiments with theory and numerical results. *International Journal of Heat and Mass Transfer*, **48**(25-26):5580-5601. [doi:10.1016/j.ijheatmasstransfer.2005.05.041]

Ho, C.M., Tai, Y.C., 1998. Micro-electronic-mechanic-systems (MEMS) and fluid flows. *Annual Review of Fluid Mechanics*, **30**(1):579-612. [doi:10.1146/annurev.fluid.30.1.579]

Hung, Y.M., 2009. A comparative study of viscous dissipation effect on entropy generation in single-phase liquid flow in microchannels. *International Journal of Thermal Sciences*, **48**(5):1026-1035. [doi:10.1016/j.ijthermalsci.2008.07.011]

Husain, A., Kim, K.Y., 2008. Optimization of a microchannel heat sink with temperature dependent fluid properties. *Applied Thermal Engineering*, **28**(8-9):1101-1107. [doi:10.1016/j.applthermaleng.2007.12.001]

Incropera, F.P., Dewitt, D.P., Bergman, T.L., Lavine, A.S., 2007. Introduction to Heat Transfer (5th Ed.). Wiley, New York, p.137-145.

Jeong, H.E., Jeong, J.T., 2006. Extended Graetz problem including streamwise conduction and viscous dissipation in microchannels. *International Journal of Heat and Mass Transfer*, **49**(13-14):2151-2157. [doi:10.1016/j.ijheatmasstransfer.2005.11.026]

Kim, D.K., Kim, S.J., 2006. Averaging approach for microchannel heat sinks subject to the uniform wall temperature condition. *International Journal of Heat and Mass Transfer*, **49**(3-4):695-706. [doi:10.1016/j.ijheatmasstransfer.2005.08.012]

Kim, S.J., Kim, D., 1999. Forced convection in microstructures for electronic equipment cooling. *ASME Journal of Heat Transfer*, **121**(3):639-645. [doi:10.1115/1.2826027]

Knight, R.W., Goodling, J.S., Hall, D.J., 1991. Optimal

thermal design of forced convection heat transfer—Analytical. *ASME Journal of Electronic Packaging*, **113**(3):313-321. [doi:10.1115/1.2905412]

Koo, J., Kleinstreuer, C., 2004. Viscous dissipation effects in microtubes and microchannels. *International Journal of Heat and Mass Transfer*, **47**(14-16):3159-3169. [doi:10.1016/j.ijheatmasstransfer.2004.02.017]

Lahjomri, J., Oubarra, A., 1999. Analytical solution of the Graetz problem with axial conduction. *ASME Journal of Heat Transfer*, **121**(4):1078-1083. [doi:10.1115/1.2826060]

Maranzana, G., Perry, I., Maillet, G., 2004. Mini- and micro-channels: influence of axial conduction in the walls. *International Journal of Heat and Mass Transfer*, **47**(17-18):3993-4004. [doi:10.1016/j.ijheatmasstranfer.2004.04.016]

Michelsen, M.L., Villadsen, J., 1974. The Graetz problem with axial heat conduction. *International Journal of Heat and Mass Transfer*, **17**(11):1391-1402. [doi:10.1016/0017-9310(74)90140-9]

Nguyen, T.V., 1992. Laminar heat transfer for thermal developing flow in ducts. *International Journal of Heat and Mass Transfer*, **35**(7):1733-1741. [doi:10.1016/0017-9310(92)90143-G]

Tso, C.P., Mahulikar, S.P., 1998. The use of the Brinkman number for single phase forced convective heat transfer in micro-channels. *International Journal of Heat and Mass Transfer*, **41**(12):1759-1769. [doi:10.1016/S0017-9310(97)00232-9]

Tso, C.P., Mahulikar, S.P., 1999. The role of the Brinkman number in analyzing flow transitions in micro-channels. *International Journal of Heat and Mass Transfer*, **42**(10):1813-1833. [doi:10.1016/S0017-9310(98)00276-2]

Tso, C.P., Mahulikar, S.P., 2000. Experimental verification of the role of the Brinkman number in micro-channels using local parameters. *International Journal of Heat and Mass Transfer*, **43**(10):1837-1849. [doi:10.1016/S0017-9310(99)00241-0]

Tuckerman, D.B., Pease, R.F.W., 1981. High-performance heat sinking for VLSS. *IEEE Electron Device Letters*, **2**(5):126-129.

Weigand, B., Lauffer, D., 2004. The extended Graetz problem with piecewise constant wall temperature for pipe and channel flows. *International Journal of Heat and Mass Transfer*, **47**(24):5303-5312. [doi:10.1016/j.ijheatmasstransfer.2004.06.027]

Zhao, C.Y., Lu, T.J., 2002. Analysis of microchannel heat sink for electronics cooling. *International Journal of Heat and Mass Transfer*, **45**(24):4857-4869. [doi:10.1016/S0017-9310(02)00180-1]

2010 JCR of Thomson Reuters for *JZUS-A* and *JZUS-B*

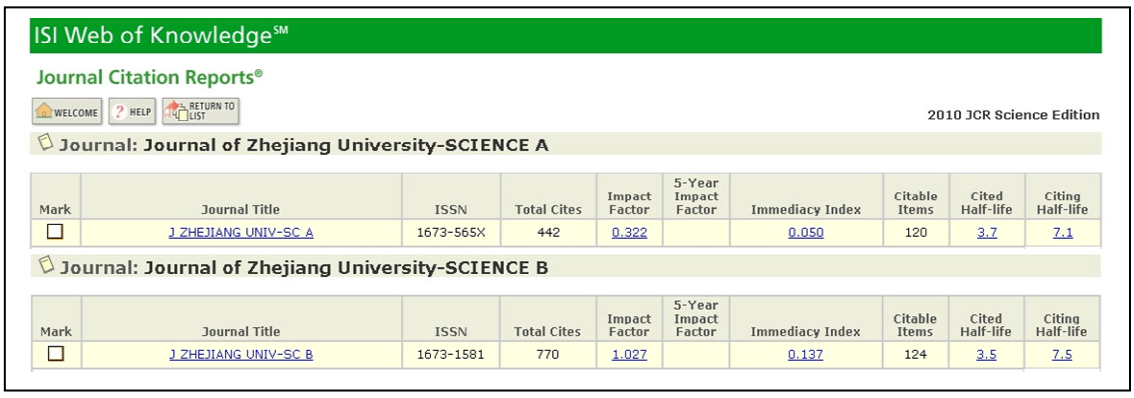

ISI Web of Knowledge℠

Journal Citation Reports®

WELCOME | HELP | RETURN TO LIST

2010 JCR Science Edition

Journal: Journal of Zhejiang University-SCIENCE A

Mark	Journal Title	ISSN	Total Cites	Impact Factor	5-Year Impact Factor	Immediacy Index	Citable Items	Cited Half-life	Citing Half-life
☐	J ZHEJIANG UNIV-SC A	1673-565X	442	0.322		0.050	120	3.7	7.1

Journal: Journal of Zhejiang University-SCIENCE B

Mark	Journal Title	ISSN	Total Cites	Impact Factor	5-Year Impact Factor	Immediacy Index	Citable Items	Cited Half-life	Citing Half-life
☐	J ZHEJIANG UNIV-SC B	1673-1581	770	1.027		0.137	124	3.5	7.5